RLC effects in fine pitch anisotropic conductive film connections

G. Dou
Wolfson School of Mechanical and Manufacturing Engineering, Loughborough University, Loughborough, UK

Y.C. Chan
Department of Electronic Engineering, City University of Hong Kong, Kowloon, Hong Kong, People's Republic of China

J.E. Morris
Electrical and Computer Engineering, Portland State University, Portland, Oregon, USA, and

D.C. Whalley
Wolfson School of Mechanical and Manufacturing Engineering, Loughborough University, Loughborough, UK

Abstract

Purpose – The resistance, capacitance and inductance of anisotropic conductive film (ACF) connections determine their high frequency electrical characteristics. The presence of capacitance and inductance in the ACF joint contributes to time delays and cross-talk noise as well as simultaneous switching noise within the circuit. The purpose of this paper is to establish an experimental method for estimating the capacitance and inductance of a typical ACF connection. This can help to provide a more detailed understanding of the high frequency performance of ACF assemblies.

Design/methodology/approach – Experiments on the transient response of an ACF joint were performed using a digital oscilloscope capable of achieving the required ns resolution. An equivalent circuit model is proposed in order to quantify the capacitance (C) and inductance (L) of a typical ACF connection and this model is fitted to the experimental data. The full model consisted of two resistors, an inductor, and a capacitor.

Findings – The capacitance and inductance of a typical ACF connection were estimated from the measured transient response using Kirchhoff's voltage law. The method for estimation of R, L, and C from the transient response is discussed, as are the RLC effects on the high frequency electrical characteristics of the ACF connection.

Research limitations/implications – There was decay time deviation between the calculation and the experiment. It may have resulted from the skin effect in the high frequency response and the adhesive surrounding joint as well. The main reason may be the capacitance zctric lost. Further research work will be done to determine more accurately the dielectric losses in anisotropic conductive adhesive (ACA) joint.

Originality/value – This paper presents a new method to characterise the high frequency properties of ACA interconnections and will be of use to engineers evaluating the performance of ACF materials in high frequency applications.

Keywords Dielectric properties, Frequencies, Electrical conductivity, Capacitance, Inductance

Paper type Research paper

Introduction

The use of anisotropic conductive adhesives (ACAs) provides a simple method for creation of high density interconnections (Liu, 1999). Industrial applications of ACAs have become increasingly common over the last two decades (Liu, 2001). They offer advantages in terms of low assembly temperature, higher component density, and reduced package size (Dudek *et al.*, 1999). ACAs have been used in fine pitch packaging applications such as flip chip die-attach and LCD display assembly. ACAs are commonly used in the form of pre-formed films, referred to as anisotropic conductive films (ACFs).

Conductive adhesives are of increasing interest for future electronics assembly for high-frequency applications. There have been a number of previous studies of the high frequency performance of ACF bonding. For example, Dernevik *et al.* (1997) and Shilbom *et al.* (1998) measured the performance of ACF bonded test structures and showed that their transmission performance in the range of 40 MHz-21 GHz is similar to that of solder, and Yim *et al.* (1999) showed acceptable performance of ACFs up to 13 GHz.

Several high frequency models of ACF joints have also been developed. For example, Ahn *et al.* (1999) and Yim *et al.* (1999) proposed equivalent circuit models of the ACF joint, consisting of resistors, R, inductors, L, and capacitors, C. Ryu *et al.* (2000)

used a genetic algorithm to fit such a model to the measured impedances. However, although such experiments and modelling have been undertaken, the models do not always adequately fit the results. Although the series resistance of a connection can be measured, direct measurement of the R, L, and C of the equivalent circuit cannot be made. However, in theory the R and LC product of the equivalent circuit can be calculated from the transient response to a square wave voltage input. In this paper, the transient electrical response of a single type of ACF, consisting of resin cored conductor particles coated with nickel and gold layers and carried in an epoxy resin matrix, is investigated and from the measurement results the values of R, L, and C for the ACF joint equivalent circuit were estimated.

Experimental method

Chip and substrate interconnection patterns

The area of the experimental chip was 3×11 mm, with 60 groups of bumped bond pads arranged around the periphery. Each group consists of five bumps with a height of $4\,\mu$m and area of $50 \times 70\,\mu$m. Figure 1 shows a group of bumps on the chip. The bump pitch/spacing was $70\,\mu$m. Three of the bumps are connected by an Al film for joint resistance measurement using the four points probe (FPP) method. The other two bumps are designed for insulation resistance measurements and are not connected.

Flex substrates (Au/Ni/Cu on Upilex) were used in this experiment. The trace pattern corresponding to the chip bond pad group in Figure 1 is shown in Figure 2.

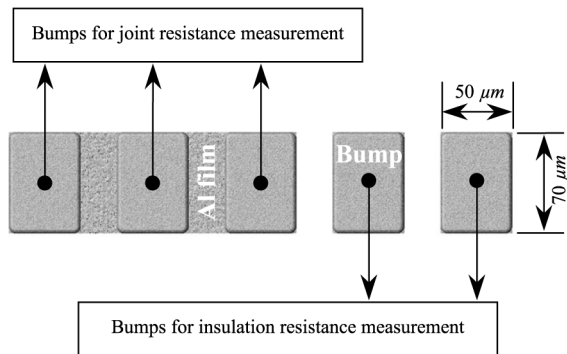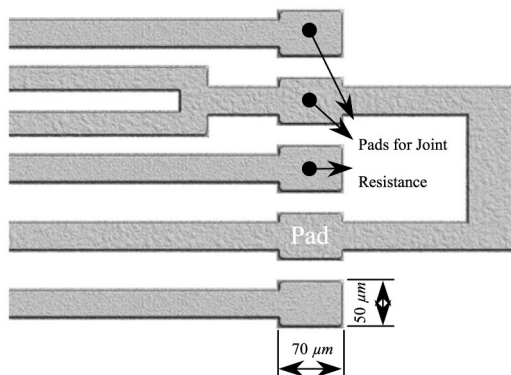**Figure 1** A group of bumps on the chip

Figure 2 A group of pads on the substrate

ACF material

The ACF studied in the experiment employs a random dispersion of conductive particles. It was a commercially available material designed for fine pitch interconnection. The manufacturer's data gave the diameter of the ACF particles to be $3.5\,\mu$m and the particle density to be 3.5 million/mm^3. This resulted in a particle density on the pads of about 5×10^3/mm^2.

Bonding process

All of the chips and substrates were carefully cleaned using ethanol prior to bonding in order to remove any contaminants. ACF preforms were cut into the correct size for pre-bonding. Two flip chip bonding machines, a Karl Suss 9493 Mauren and a Toray (FC1200-2k-#95) were used for pre-bonding and final bonding, respectively. The bonding parameters are summarized in Table I and were selected according to the ACF specification. Pre-bonding was used to laminate the ACF onto the substrate, followed by final bonding of the chip onto the substrate at a pressure of 100 MPa and temperature of $180°$C.

FPP resistance measurement

Figure 3 shows a group of ACF joints. There are five ACF joints in a group designed for electrical measurement using the four wire or FPP method. Traces 1 and 5 are connected to a current source, while traces 3 and 4 are connected to an oscilloscope or multi-meter for voltage measurement.

The arrangement for measurement of the electrical response of joint 2 is schematically shown in Figure 4(a). The joint can be represented by the equivalent circuit in Figure 4(b), which is developed from that presented by Ahn *et al.* (1999). For DC conditions R_1 is due to the series resistance of the chip bump and the substrate pad, while R_2 represents the resistance of the ACF particles trapped in the joint between the bump and the pad. However, under AC conditions R_2 may also include other effects, such as dielectric losses. C and L are the capacitance and inductance of the ACF between the bump and the pad.

Table I Bonding parameters for the ACF Joints

Bonding process	Temperature (°C)	Pressure (MPa)	Time (s)
Pre-bonding	80	10	5
Final bonding	180	100	15

Figure 3 A group of ACF joints
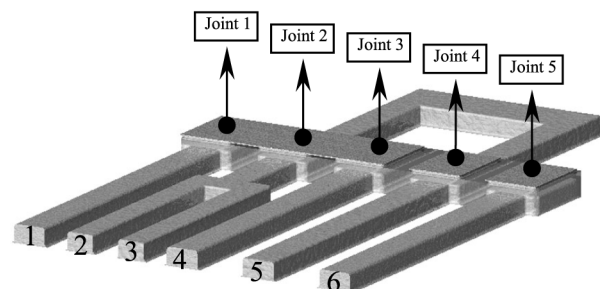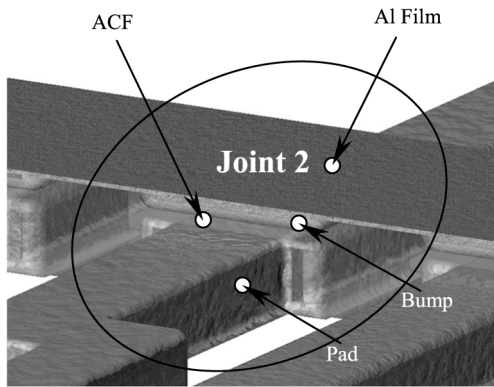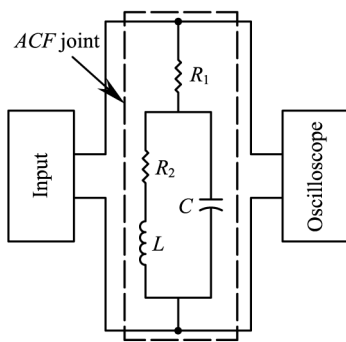
Figure 4

(a) Structure of joint 2

(b) Joint 2's equivalent circuit

Electrical measurement system

Figure 5 shows the configuration of the experimental system for DC resistance measurement of the ACF joints. A voltage source is connected to traces 1 and 5, and a voltmeter is connected to traces 3 and 4 as shown in Figure 3. VR is a variable resistor used for accurately setting the test current, which is measured by the ammeter, A.

The experimental configuration shown in Figure 6 was used to determine the *RLC* response of the ACF joints to a square wave input signal. A voltage square wave signal was supplied by a function generator via a DS0026 current amplifier, VR is a variable resistor as before. A 1 K resistor and a 100 pF capacitor were used to filter the input to the current amplifier. A Tektronix TDS 3014 digital oscilloscope was used for data

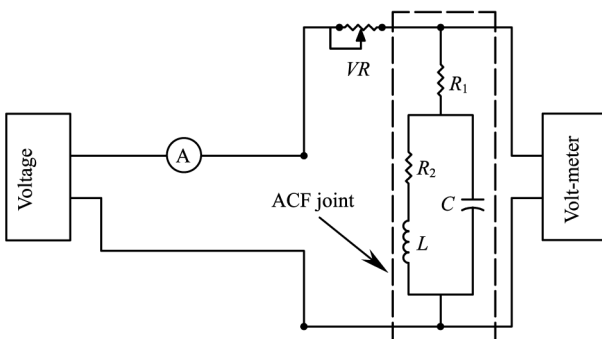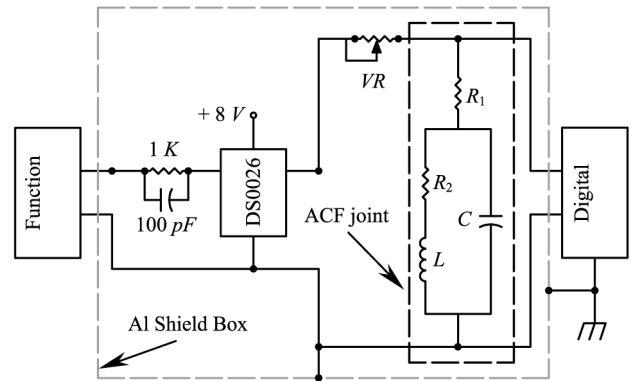**Figure 5** Experimental configuration for the DC joint resistance measurements

Figure 6 Experimental configuration for the *RLC* response measurement

acquisition. In order to shield out noise, an aluminium shielding box was used to enclose the amplifier circuitry and the test specimen. All of the ground terminals (including the equipment ground) were connected to this box.

A 10 MHz signal was used in this work, due to the capabilities of the oscilloscope available. This frequency is low compared with modern RF and digital circuit applications, but was considered sufficient to establish the validity of the proposed measurement technique.

Theory

For a constant current, the capacitance and inductance in a joint do not affect its impedance, however, for a rapidly varying current input, such as in RF or high speed digital circuits, the stray capacitances and inductances present within the joint may result in distortion of the signal. These distortion effects typically include signal attenuation and cross-talk between adjacent conductors but, particularly in digital circuits, the distortion may be apparent as a time delay after any step change in input current before the output signal becomes stable. Where both inductive and capacitive parasitics are significant there may be a transient oscillatory component to this transient response, sometimes known as ringing. This phenomenon is also called the *RLC* response. The values of *L* and *C* predominantly determine the frequency of this ringing, whilst the value of *R* controls the rate of decay, or damping, of the oscillations.

The series resistance of a joint can be directly measured at low frequency, however, at high frequency there may effectively be additional resistive losses due to, for example, current crowding due to the skin effect and the dissipation of energy in the dielectric of any stray capacitances.

The parasitic capacitance of an ACF joint can be assumed to be primarily due to the layer of adhesive resin forming the bulk of the joint area, which is effectively the dielectric layer in a parallel plate capacitor formed by the two contacts being interconnected and as will be seen later this capacitance can be estimated from the known geometry and materials. The physical original of the inductance of the ACF joint is more complicated as it involves the joint, the contact areas, the bump, the pad and the particles, and is therefore, much more difficult to calculate from first principles. However, it can be estimated from the *RLC* response using the relationship between *L*, *C* and the period of the oscillations, *T*.

Equations for the *RLC* response

By considering the *RLC* circuit shown in Figure 7 with a current input $i(t)$ and voltage output $y(t)$, we may obtain three differential equations by applying Kirchhoff's voltage law around the loop indicated by $i(t)$.

$$y(t) = v_c(t) \qquad (1)$$

$$C\frac{dv_c(t)}{dt} = i(t) - i_L(t) \qquad (2)$$

$$L\frac{di_L(t)}{dt} = v_c(t) - Ri_L(t) \qquad (3)$$

From equations (1)-(3), a second-order differential equation can be derived to relate $y(t)$ and $i(t)$.

$$\frac{d^2y(t)}{dt^2} + \frac{R}{L}\frac{dy(t)}{dt} + \frac{1}{LC}dy(t) = \frac{R}{LC}i(t) \qquad (4)$$

The solution to equation (4) may or may not be oscillatory, depending on the relative magnitudes of *R*, *L* and *C*, but Figure 8 shows a classic oscillatory or under-damped *RLC*

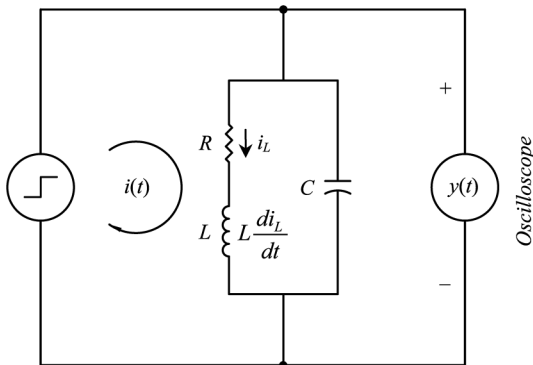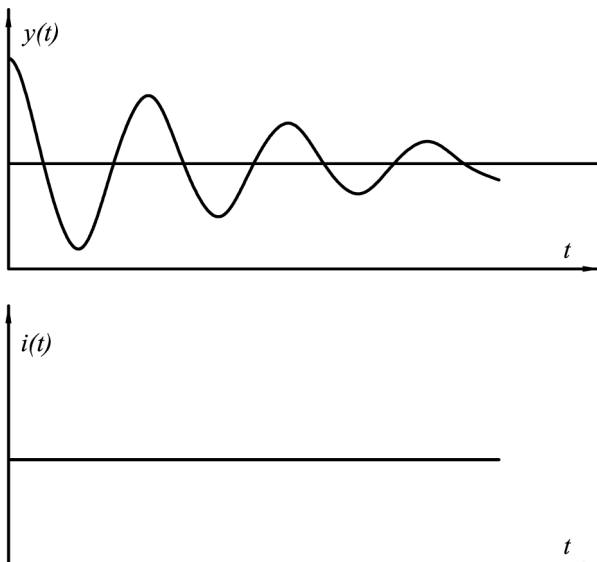**Figure 7** *RLC* circuit to illustrate the derivation of the input-output relationship

Figure 8 *RLC* response to a step input

voltage response profile for the circuit shown in Figure 7. For such an under-damped situation to occur:

$$\left(\frac{R}{L}\right)^2 - \frac{4}{LC} < 0 \qquad (5)$$

For the step input $i(t)$ in Figure 8, the oscillatory form of the complementary function of the differential equation (4), is:

$$y(t) = e^{-\alpha t}\{A\cos\beta \cdot t + B\sin\beta \cdot t\} + Ri(t) \qquad (6)$$

The characteristic equation of equation (4) is:

$$\lambda^2 + \frac{R}{L}\lambda + \frac{1}{LC} = 0 \qquad (7)$$

which has the complex roots:

$$\lambda_1, \lambda_2 = \alpha \pm \beta.j = \frac{-\frac{R}{L} \pm \sqrt{\frac{4}{LC} - \left(\frac{R}{L}\right)^2}\,j}{2} \qquad (8)$$

Hence, equation (6) can be written as:

$$y(t) = e^{-(R/2L)t}\left\{A\cos\left[\frac{1}{2}\sqrt{\frac{4}{LC} - \left(\frac{R}{L}\right)^2}\right]t \right.$$
$$\left. + B\sin\left[\frac{1}{2}\sqrt{\frac{4}{LC} - \left(\frac{R}{L}\right)^2}\right]t\right\} + Ri(t) \qquad (9)$$

or

$$y(t) = \sqrt{A^2 + B^2}\,e^{-(R/2L)t}\sin\left\{\left[\frac{1}{2}\sqrt{\frac{4}{LC} - \left(\frac{R}{L}\right)^2}\right]t + actg\left(\frac{A}{B}\right)\right\}$$
$$+ Ri(t) \qquad (10)$$

From equation (10), we can obtain the period of the transient response:

$$T = \frac{2\pi}{\beta} = \frac{4\pi}{\sqrt{\frac{4}{LC} - \left(\frac{R}{L}\right)^2}} \qquad (11)$$

Equation (11) can be rearranged to allow calculation of the inductance given *T*, *R* and *C*:

$$L^2 - \frac{T^2}{4\pi^2 C}L + \frac{R^2 T^2}{16\pi^2} = 0 \qquad (12)$$

However, for the experimental values found in this work:

$$R^2 T^2 \ll 16\pi^2 \qquad (13)$$

Thus, equation (12) can be approximated as:

$$L^2 - \frac{T^2}{4\pi^2 C}L = 0 \qquad (14)$$

which gives:

$$L = \frac{T^2}{4\pi^2 C} \qquad (15)$$

Moreover, the period and the frequency *f* of the response are given by:

$$T = 2\pi\sqrt{LC}, \quad f = \frac{1}{2\pi\sqrt{LC}} \qquad (16)$$

The rate of decay of the oscillations described by equation (9) is characterised by the time constant $2L/R$, i.e. the oscillations

will have fallen to 37 percent (e^{-1}) of their initial magnitude after a time of $2L/R$.

Estimation of the capacitance of an ACF joint

In order to estimate the parasitic capacitance of an ACF joint it can be considered as an ideal, parallel plate capacitor, consisting of a slab of insulating material with dielectric constant, e, between two perfectly conducting plates as shown in Figure 9. In this instance the plates are the substrate and chip bond pads.

The capacitance, C, of the ACF joint is, therefore:

$$C = \frac{\varepsilon_r \varepsilon_0 wl}{d} \quad (17)$$

where ε_r, dielectric constant of the slab material; d, distance between the plates (m); w, width of the slab (m); and l, length of the slab (m).

For the experiment parameters used in the bonding process the transformation (degree of compression) of the ACF particles is to about 60 percent of their original diameter of $3.5\,\mu m$, and thus the distance, d, between the plates is about $2\,\mu m$ (Dou *et al.*, 2003). For the ACF joint used in the experiment, the other values are $w = 50\,\mu m$, $l = 70\,\mu m$ and $\varepsilon_r = 4.5$, whilst $\varepsilon_0 = 4.5 \times 8.85 \times 10^{-12}$ F/m. Hence using equation (17) the capacitance of the joint is calculated to be:

$$C = 6.97 \times 10^{-2} \text{ pF} \quad (18)$$

Estimation of the substrate and chip pad resistance

Although the FPP resistance measurement method prevents interconnection resistances affecting the measured resistance, the substrate and chip pads are in series with the ACF connection and their resistance, therefore, needs to be considered. The total DC resistance of an ACF joint, therefore, consists of five parts, as shown in Figure 10 (Dou *et al.*, 2003). These are the resistances of the chip bump and PCB pad, R_{bump} and R_{pad}, the resistance of the conductive particles $R_{particles}$, and the contact resistances between the particles and bump or pad $R_{contact}$ $R_{contact} + R_{particles} + R_{contact}$ will clearly consist of the parallel resistances through all of the conductor par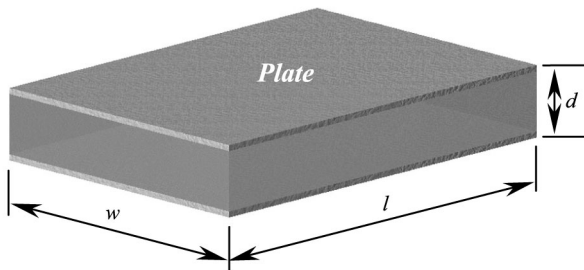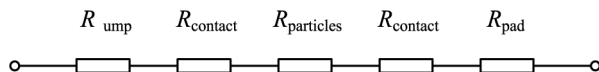ticles present within the individual connection area. The conduction mechanisms for the contact resistance are complicated and are still poorly understood, because they result from a mechanical rather than metallurgical contact (Oguibe *et al.*, 1998). Many factors can affect the contact resistance, such as the nature of the contact surface, thermal stress, deformation degree, etc.

The structure of the chip bump and substrate bond pad metallization used in the experiment is shown in Figure 11. Each chip bump consisted of three layers, an Al film, a Ni layer and an Au layer. The Al film and Ni layer are slabs, but the Au layer is very thin. In order to simplify estimation of the resistance of the Au layer, it is also assumed as a slab. The pad metallization also had three parts, a Cu layer, a Ni layer and an Au layer as shown in Figure 9(b). Both the Ni layer and the Au layer are thin, and are also assumed to be slabs for the estimation of the pad resistance.

The resistance, R, of each layer can be calculated using:

$$R = \frac{d}{\sigma wl}\,\Omega \quad (19)$$

The dimensions and calculated resistances of each of the bump and the pad layers are shown in Table II. The individual slab resistances are in series, so the total resistance of the bump is:

$$R_{bump} = 7.58 \times 10^{-3} + 7.24 \times 10^{-2} + 3.16 \times 10^{-3}$$
$$= 8.31 \times 10^{-2}\,m\Omega \quad (20)$$

and that of the pad is:

$$R_{pad} = 7.38 \times 10^{-2} + 1.02 \times 10^{-1} + 3.16 \times 10^{-3}$$
$$= 1.79 \times 10^{-1}\,m\Omega \quad (21)$$

R_1 in Figure 4(b) is the combined resistance of the bump and the pad in the ACF joint, therefore, R_1 is:

$$R_1 = R_{bump} + R_{pad} \quad (22)$$

Figure 11 Construction of the connections and their approximation (a) chip bumps; (b) substrate pads

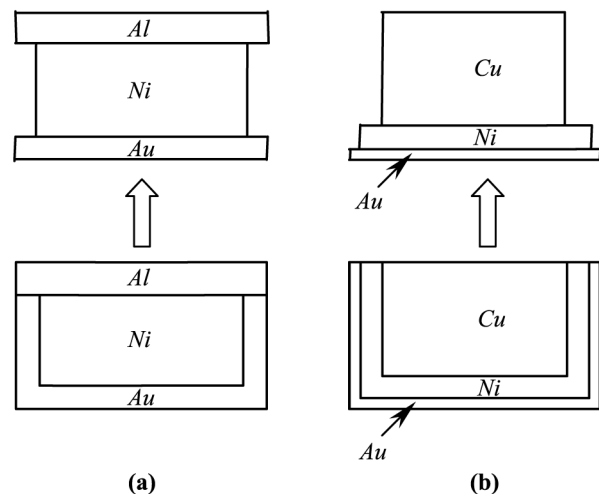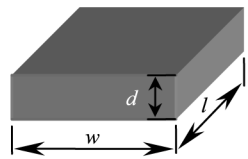**Figure 9** Classical parallel plate capacitor

Figure 10 DC equivalent circuit of the ACF joint

Table II Bump and pad resistances for the ACF joint

Slab geometry

	Material	Length, l (μm)	Width, w (μm)	Height, d (μm)	Conductivity, s (/$\mu m \cdot O$)	Resistance (mO)
Bump	Al	70	50	1	37.7	7.58E-3
	Ni	69	49	3.5	14.3	7.24E-2
	Au	70	50	0.5	45.2	3.16E-3
Pad	Cu	70	39	12	59.6	7.38E-2
	Ni	70	49	5	14.3	1.02E-1
	Au	70	50	0.5	45.2	3.16E-3

Substituting the previously calculated values into equation (17), the estimated value of R_1 is:

$$R_1 = R_{bump} + R_{pad} = 0.262\,\text{m}\Omega$$

Experimental results

First, the DC resistance of a single ACF joint was measured and for a 1 mA test current the voltage drop was found to be 0.040 mV equating to a resistance of 40 mΩ. This is much larger than the previously calculated value for R_1, i.e.

$$R_1 \ll R_{joint}$$

Therefore, R_1 contributes little to the joint resistance, and can be ignored during further consideration of the *RLC* response. As defined in Figure 4(b), resistance R_2 results from conduction through the contact areas and the metal layers of the particles. The resistance of one ACF joint has been estimated to vary from 2 to 6 mΩ if the particles deformation degree is more than 30 percent (Dou *et al.*, 2003). This shows that the DC resistance of the joint is dominated by the contact resistances between the particles and the bump/pad.

Second, the *RLC* response of the ACF joint was captured. The Figure 12(a) and (b) show the input signal and *RLC* response, respectively. The input current was 0-7 mA peak to peak for VR set to 1 kΩ and the frequency of the test signal was 10 MHz.

Figure 13 shows the measured voltage response on an expanded time axis. The response plotted is the mean of 16 acquisitions by the digital oscilloscope. If we consider $i(t)$ to be a step input for simplicity, Figure 13 can be considered as a classic *RLC* response as shown in Figure 8.

The frequency of oscillation can be measured from the time between the signal crossing the steady state voltage, which is slightly above zero due to the DC resistance of the joint. The accuracy of this measurement is improved by averaging over several cycles and in Figure 14 it can be seen that there are five whole cycles between the zero crossings at 16.4 and 30.4 ns.
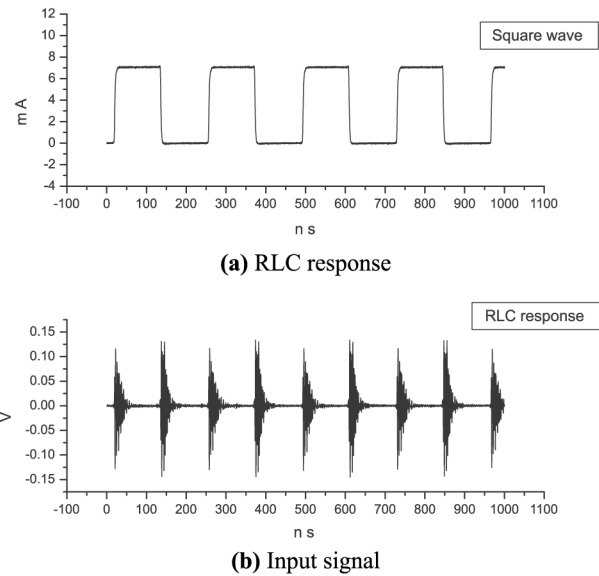
Figure 12

(a) RLC response

(b) Input signal

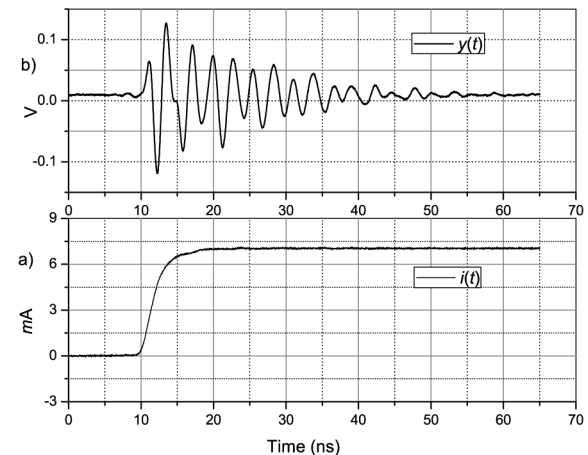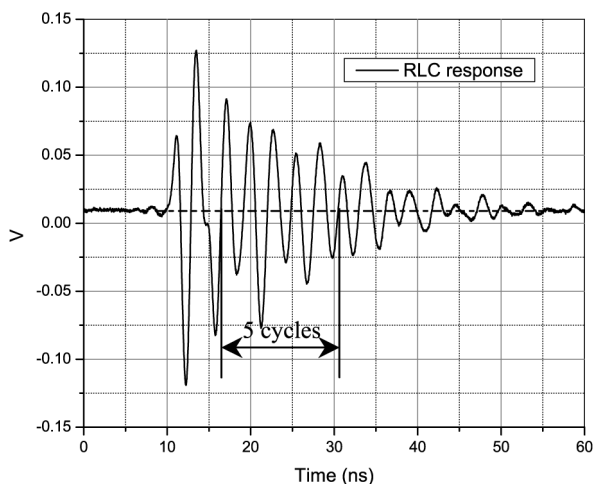**Figure 13** Averaged voltage response and input current

Figure 14 *RLC* response for period counting

From this, the period of the RLC transient response is:

$$T = \frac{30.4 - 16.4}{5}\,\text{ns} = 2.8\,\text{ns}$$

and the frequency is therefore:

$$f = \frac{1}{T} = 357\,\text{MHz}$$

Substituting the measured value for T and the previously calculated value of C into equation (15), we obtain L:

$$L = \frac{T^2}{4\pi^2 C} = \frac{(2.8 \times 10^{-9})^2}{4\pi^2 \times 6.97 \times 10^{-14}} = 2.85\,\mu\text{H}$$

The observed RLC decay time, τ, is around 30 ns, as shown in Figure 14, however, the decay time derived from equation (10) is $2L/R_2$, i.e. 0.14 ms, which is about 5,000 times longer than the observed. This suggests that there are significant additional resistive losses in the joint at high frequencies, which have not been accounted for in the model so far developed. One possibility is that this discrepancy may result from the skin effect however, at the frequencies of interest they are over 3 μm and a more likely explanation is considered to be the dielectric losses in the joint capacitance. From the experimental results equation (10) may be used to estimate the series resistance of the joint (as shown in Figure 7) at high frequency as:

$$R = \frac{2L}{\tau} = \frac{2 \times 2.85 \times 10^{-6}}{30 \times 10^{-9}} = 190\,\Omega$$

Thus, the equivalent parallel resistance R_p can be written as:

$$R_p = \frac{R^2 + (2\pi f L)^2}{R}$$

$$= \frac{190^2 + (2\pi \times 357 \times 10^6 \times 2.85 \times 10^{-6})^2}{190} \approx 215\,\text{k}\Omega$$

Then, the dielectric dissipation factor, Tan δ, of the joint capacitance necessary to create such a parallel resistance can be calculated as:

$$\text{Tan}\,\delta = \frac{1/2\pi f C}{R_p} = \frac{1/(2\pi \times 357 \times 10^6 \times 0.0697 \times 10^{-12})}{215 \times 10^3}$$

$$\approx 2.98\,\text{percent}$$

This Tan δ figure is in line with typical dielectric losses for epoxy resins and, therefore, the decay time deviation may be largely attributable to the capacitance dielectric loss.

Conclusions

In conclusion, a detailed equivalent circuit RLC model of an ACF joint has been proposed. The model was used to predict the transient response of an ACF joint and, if the joint capacitance is first calculated from its known geometry and dielectric constant, the inductance of the joint can be calculated from the RLC response when a square wave input signal is applied. The period of the transient response equation relating to the capacitance and inductance is $T = 2\pi\sqrt{LC}$. The calculated contribution to the overall DC resistance of the ACF joint due to the bump and the pad are

much lower than the measured joint resistances, indicating most of the DC joint resistance is due to contact resistances.

For the specific materials and joint geometry studied the estimated values for the model were $R_1 = 0.3\,\text{m}\Omega$, $R_2 = 40\,\text{m}\Omega$, $C = 0.0697\,\text{pF}$, and $L = 2.85\,\mu\text{H}$. The resistances within the model do not significantly affect the period of the high frequency response and the resonant frequency of the joint should be close to the response frequency.

However, the calculated decay time is much smaller than that measured, indicating that at high frequencies the joint resistance is much higher. Analysis of this discrepancy indicates that the main cause is likely to be dielectric losses in the joint capacitance, suggesting that the adhesive dielectric properties are important to the electrical behaviour of ACF joints at high frequencies. Direct measurement of the dielectric losses of adhesive resins will be required to confirm this finding.

References

Ahn, S., Ryu, W., Yim, M-J., Lee, J., Jeon, Y-D.W., Kim, W., Paik, K-W. and Kim, J. (1999), "Over 10 GHz equivalent circuit model of ACF flip-chip interconnect using Ni-filled ball and Au-coated polymer balls", Proceedings of the 24th IEEE/CPMT International on Electronics Manufacturing Technology Symposium, Austin, Texas, USA, pp. 421-5.

Dernevik, M., Shilbom, R., Lai, Z., Starski, P. and Liu, J. (1997), "High-frequency measurement and modelling of anisotropic electrically conductive adhesive flip-chip joint", Advances in Electronic Packaging, Proceedings of the ASME INTERpack Conference, Kohala Coast, Hawaii, EEP-Vol. 19-1, pp. 177-84.

Dou, G.B., Chan, Y.C. and Liu, J. (2003), "Electrical conduction characteristics of anisotropic conductive adhesive particles", Journal of Electronic Packaging, Transactions of the ASME, Vol. 125, pp. 609-16.

Dudek, R., Meinel, S., Schubert, A., Michel, B., Dorfmüller, L., Knoll, P.M. and Baumbach, J. (1999), "Flow characterization and thermo-mechanical response of anisotropic conductive films", IEEE Transactions On Components and Packaging Technology, Vol. 22 No. 2, pp. 177-85.

Liu, J. (1999), Conductive Adhesive for Electronics Packaging, Electrochemical Publications Ltd, British Isles.

Liu, J. (2001), "ACA bonding technology for low cost electronics packaging applications – current status and remaining challenges", Soldering & Surface Mount Technology, Vol. 13 No. 3, pp. 39-57.

Oguibe, C.N., Mannan, S.H., Whalley, D.C. and Williams, D.J. (1998), "Conduction mechanisms in anisotropic conducting adhesive assembly", IEEE Transactions on Components, Packaging and Manufacturing Technology – Part A, Vol. 21 No. 2, pp. 235-42.

Ryu, W., Jin, M., Ahm, S., Lee, J., Kim, W., Paik, K.W. and Kim, J. (2000), "High-frequency SPICE model of anisotropic conductive film flip-chip interconnections based on a genetic algorithm", IEEE Transactions On Components and Packaging Technology, Vol. 23 No. 3, pp. 542-5.

Shilbom, R., Dernevik, M., Lai, Z., Starski, P. and Liu, J. (1998), "Conductive adhesive for high-frequency applications", IEEE Transactions on Components, Packaging, and Manufacturing Technology – Part A, Vol. 21 No. 3, pp. 469-77.

Yim, M-J., Ryu, W., Jeon, Y-D., Lee, J., Ahn, S. and Paik, K-W. (1999), "Microwave model of anisotropic conductive film flip-chip interconnections for high frequency applications", *IEEE Transactions on Components, Packaging, and Manufacturing Technology*, Vol. 22, pp. 575-81.

About the authors

G. Dou earned his BE and ME degrees in Materials Engineering from Harbin Institute of Technology in 1999 and 2001, respectively, and is currently a PhD student in the Wolfson School of Mechanical and Manufacturing Engineering, Loughborough University. From 2002 to 2003, he was a Research Assistant in the Department of Electronic Engineering, City University of Hong Kong. His current research interests include advanced electronics packaging and assemblies, and particularly fine pitch electronic packaging. G. Dou is the corresponding author and can be contacted at: gb.dou@lboro.ac.uk.

Y.C. Chan earned his BSc degree in Electrical Engineering in 1977, an MSc degree in Materials Science in 1978, and a PhD degree in Electrical Engineering in 1983, all from Imperial College of Science and Technology, University of London. He then joined the Advanced Technology Department of Fairchild Semiconductor in California as a Senior Engineer, where he worked on integrated circuit technology. In 1985, he was appointed to a Lectureship in Electronics at the Chinese University of Hong Kong. Between 1987 and 1991, he worked in various senior operations and engineering management functions in electronics manufacturing (including SAE Magnetics (HK) Ltd and Seagate Technology). He also set up the Failure Analysis and Reliability Engineering Laboratory for SMT PCBs in Seagate Technology (Singapore). He joined City Polytechnic of Hong Kong (now City University of Hong Kong) as a Senior Lecturer in Electronic Engineering in 1991. After three promotions within CityU, he is currently Chair Professor and Director of the EPA Centre, and Assistant Head for Applied Research and Public Relations in the Department of Electronic Engineering. He has authored or co-authored over 100 scientific publications in peer-reviewed journals and over 50 international conference papers. His current research interests include advanced electronic packaging and assemblies, failure analysis, and reliability engineering.

J.E. Morris is a Professor of Electrical and Computer Engineering at Portland State University, Oregon, Professor Emeritus at the State University of New York at Binghamton, and an IEEE fellow. His BSc and MSc (with 1st Class Honours in Physics) degrees are from the University of Auckland, New Zealand, and the PhD in Electrical Engineering is from the University of Saskatchewan, Canada. He has served as Department Chair at both Binghamton and Portland, and was the first Director of Binghamton's Institute for Research in Electronics Packaging. Professor Morris was Treasurer of the IEEE Components, Packaging, and Manufacturing Technology Society from 1991 to 1997, Vice-President for Conferences from 1998 to 2003, and is now an IEEE-CPMT Distinguished Lecturer. He is an Associate-Editor of the *IEEE Transactions on Components and Packaging Technology*, with responsibility for Adhesives, and has edited three books on electronics packaging. His research activities are currently focused on electrically conductive adhesives and the electrical conduction mechanisms in discontinuous thin metal films, with application to single-electron transistor nanoelectronics. He is also actively involved in the promotion of international educational exchanges, and in internet education.

D.C. Whalley is a Senior Lecturer within the Interconnection Research Group at Loughborough University, the UK's leading university research team addressing the design, manufacture and reliability of electronics packaging and interconnection. His research primarily focuses in areas such as the development and simulation of electronics assembly processes, such as soldering and adhesive bonding. This research has led to over 100 refereed conference and journal papers, together with numerous other publications, reports and contributions to books. He previously worked as a Research Engineer at the Lucas Automotive Advanced Engineering Centre and as a Visiting Professor at Chalmers University of Technology in Göteborg, Sweden and at Nanyang Technological University, Singapore. David is Editor in Chief of *Soldering & Surface Mount Technology* and is an Associate Editor of the *IEEE Transactions on Components, Packaging and Manufacturing Technology: Electronic Packaging Manufacturing*. He also serves on the organizing committees of a number of international conferences. He is a Chartered Electrical Engineer and a senior member of the IEEE.